



Article

Impact of Land Use and Land Cover Change on Soil Erosion in Dondor Watershed, Blue Nile Basin, Northwestern Ethiopia

Liyew Birhanu ^{1,2,*}, Yared Mekonen ¹, Abineh Tilahun ³, Nigussie Amsalu ¹ and Heiko Balzter ^{2,4}

- Department of Biology, Debre Markos University, Debre Markos P.O. Box 269, Ethiopia; 18230871ym@gmail.com (Y.M.); nigussieam2000@gmail.com or nigussie_amsalu@dmu.edu.et (N.A.)
- School of Geography, Geology and the Environment, Institute for Environmental Futures, University of Leicester, Space Park Leicester, 92 Corporation Road, Leicester LE4 5SP, UK; hb91@leicester.ac.uk
- Department of Geography, Debre Markos University, Debre Markos P.O. Box 269, Ethiopia; ababineh@gmail.com or abinehtilahun@dmu.edu.et
- ⁴ National Centre for Earth Observation, University of Leicester, Space Park Leicester, 92 Corporation Road, Leicester LE4 5SP, UK
- * Correspondence: liyewmtu@gmail.com or liyew_birhanu@dmu.edu.et

Abstract: Understanding how land use and land cover (LULC) changes affect soil erosion is essential for effective management of watershed areas. This study used Geographic Information Systems (GISs) and the Revised Universal Soil Loss Equation (RUSLE) model to analyze the impact of LULC changes on soil erosion in the Dondor Watershed. Remote sensing data, including Landsat and Sentinel-2 satellite images, alongside field surveys, topographic data, rainfall, and soil data were used. The results showed agricultural land as the primary LULC type, increasing from 43.49% in 2002 to 59.10% in 2023. Forest and built-up areas also expanded, while grassland decreased. Soil erosion estimates revealed that more than 85% of the watershed experienced very slight erosion though the average annual soil loss increased from 4.98 t ha⁻¹ year⁻¹ in 2002 to 7.96 t ha⁻¹ year⁻¹ in 2023. Agriculture and built-up areas were identified as the primary contributors to erosion. This study underscores the importance of monitoring LULC dynamics for responsible land management and conservation efforts in the watershed.

Keywords: Dondor watershed; land use land cover change; soil erosion; RUSLE



Citation: Birhanu, L.; Mekonen, Y.; Tilahun, A.; Amsalu, N.; Balzter, H. Impact of Land Use and Land Cover Change on Soil Erosion in Dondor Watershed, Blue Nile Basin, Northwestern Ethiopia. *Sustainability* 2024, 16, 10421. https://doi.org/ 10.3390/su162310421

Academic Editor: Xiaodong Nie

Received: 3 September 2024 Revised: 4 November 2024 Accepted: 12 November 2024 Published: 28 November 2024



Copyright: © 2024 by the authors. Licensee MDPI, Basel, Switzerland. This article is an open access article distributed under the terms and conditions of the Creative Commons Attribution (CC BY) license (https://creativecommons.org/licenses/by/4.0/).

1. Introduction

The escalating rate of soil erosion, largely driven by changes in land use and land cover, has emerged as a critical concern for both researchers and policymakers [1]. These changes pose a significant global threat to biodiversity, land degradation, forest fragmentation, and Earth–atmosphere interactions. Research indicates a worldwide trend toward replacing natural forests, grasslands, and savannas with cultivated lands [2]. However, the trends of land coverage and its use vary globally, influenced by various factors such as human activities, development, and population pressures [2,3].

Land use and land cover changes are the main causes of soil erosion in high-altitude watersheds, especially in Sub-Saharan Africa [4]. Intensified agricultural practices, population growth, poverty, and inadequate land management policies have accelerated these changes [5]. Topographic factors (e.g., slope), climate variability, land cover patterns, and soil properties also play significant roles in determining soil loss rates.

Recently, there has been an increased focus on environmental changes, especially the effects of changing land cover and use of natural resources. Various human influences and natural events intensify the complex and dynamic nature of changes in land use and land cover [6]. These changes pose serious risks to the environment and the economy at a global and also local level. In Africa, between 1990 and 2010, 75 million hectares of forest were converted into agriculture, which is a particularly alarming rate of deforestation [7]. About

Sustainability **2024**, 16, 10421 2 of 19

13 million hectares of East Africa's natural forest were destroyed during those two decades, leaving the remaining forest fragmented and always in danger. In emerging economies, where livelihoods and economies are heavily reliant on land productivity, soil erosion and poor conservation practices have depleted topsoil, reducing agricultural yields and exacerbating food insecurity [8].

Ethiopia, which relies heavily on agriculture, confronts a major environmental challenge in the form of land degradation. This complex issue includes gully formation, erosion of the soil, and a decline in soil fertility, all of which pose serious threats to the country's economy and natural ecosystems [9].

One major effect of land degradation is soil erosion, which can have both direct and indirect effects. It causes water pollution in addition to the loss of productive agricultural land. This erosion is particularly pronounced in cultivated areas, highlighting the critical roles of soil cover and land management practices in mitigating its effects [10,11]. The agriculture sector, which forms the backbone of Ethiopia's economy, is disproportionately affected by land degradation. The sector's vulnerability to soil erosion highlights the critical need for sustainable land management strategies, as it contributes more than 50% of GDP, 85% of export revenue, and more than 80% of employment [12].

In many regions of Ethiopia, changes in land cover and use have a negative impact on land degradation and soil erosion [3]. These changes have contributed to an accelerated soil loss, with an estimated 1.9 billion tonnes of soil being eroded annually, particularly in the highlands [13]. Consequently, almost 27 million hectares of the Ethiopian highlands have experienced severe erosion, and over 2 million hectares have become irreclaimable. The situation is further exacerbated by population pressure and unsustainable land resource management practices [14].

The complexity of the erosion process and the lack of data available over the past decade have a major impact on the accuracy of soil erosion estimates in the Dondor watershed. Regional and national-level assessments, employing diverse methodologies from indicator-based to process-based models, further influence the estimation accuracy. A pressing concern for the Dondor community is the loss of soil due to erosion. To effectively address this issue, a comprehensive evaluation using a suitable soil loss model is crucial [15,16].

Several researchers used the revised universal soil loss equation (RUSLE) model with geographic information systems (GISs) to measure soil loss across various regions of the world [17,18]. Due to its effectiveness in highland regions and its ability to more effectively estimate yearly soil loss using fewer field data, we chose the RUSLE [19,20]. Extensive research in Ethiopia's Blue Nile basin and central highlands reveals a significant trend of agricultural expansion into forested areas, driving environmental degradation. Studies by [15,21,22] highlight the long-term consequences of this land use change. Population density, as identified by [14], exacerbates erosion risks. However, recent reforestation efforts, documented by [23] and [24], demonstrate the potential for mitigating deforestation and improving vegetation cover.

The Dondor watershed lacks a comprehensive study that addresses erosion issues and changing landscapes at the sub-watershed level. Such research could provide important new information for environmental preservation and sustainable land management. Therefore, the objective of this study is to use the Revised Universal Soil Loss Equation (RUSLE) model and Geographic Information System (GIS) to examine the geospatial and temporal changes in land use, land cover change, and soil erosion dynamics in the Dondor Watershed, Amhara Regional State, Northwestern Ethiopia. Specifically, this study aimed to (1) investigate the temporal and geospatial changes in land cover and land use in the Dondor watershed from 2002 to 2023; (2) use the RUSLE model to estimate the potential rates of soil erosion in the Dondor watershed; and (3) assess the effects of changes in land cover and land use on soil erosion.

Sustainability **2024**, 16, 10421 3 of 19

2. Materials and Methods

2.1. Description of the Study Area

The Dondor watershed is located between the Guangua and Ankesha Guagusa Districts, Awi Zone, in the Amhara Region of northwestern Ethiopia. Flowing from northeast to southwest, it is 47 km long and situated inside the Upper Blue Nine Basin. The watershed spans 18,812 hectares in size and is located between 10°50′ N to 10°58′ N and 36°30′ E to 36°45′ E (Figure 1). The Dondor watershed lies between 1501 and 2889 m above sea level (m a.s.l.). In the study area, Ethiopia's agro-climatic classification [25] includes both temperate (Weyna Dega) and cool and humid (Dega) zones. According to [26], the main categories of soils include Acrisols, Fluvisols, Gleysols, Nittosols, and rock surfaces (Figure 2).

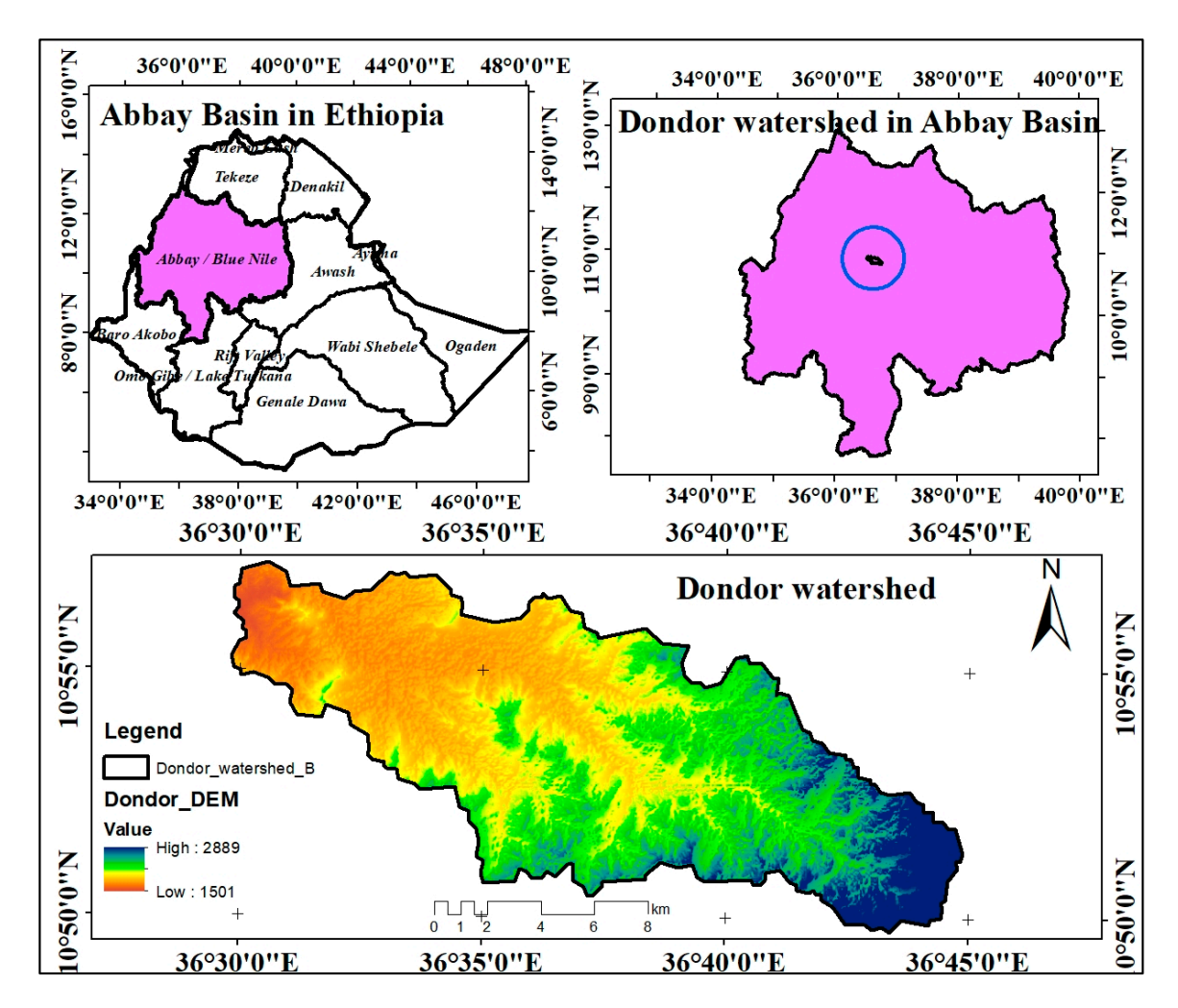


Figure 1. Location map of Dondor watershed (Source: SRTM DEM data from USGS EarthEx plorer (https://earthexplorer.usgs.gov/, accessed on 2 September 2024).

In the study area, small-scale mixed agriculture is the main agricultural practice, and it is mostly utilized for rain-fed subsistence, in which crop production is crucial. Cereals (maize, sorghum, barley, finger millet, wheat, teff), pulses (beans, soybean), and root crops (potatoes) are the primary crops cultivated. Finger millet and barley are the most prevalent. While a few farmers grow vegetables or fruits, these are typically cultivated in home gardens or irrigated areas. Livestock, including horses, donkeys, chickens, goats, lambs, and cattle, play a significant role in the agricultural system. Crop residues, private pastures, and communal grasslands provide the primary feed sources for these animals [27].

Sustainability **2024**, 16, 10421 4 of 19

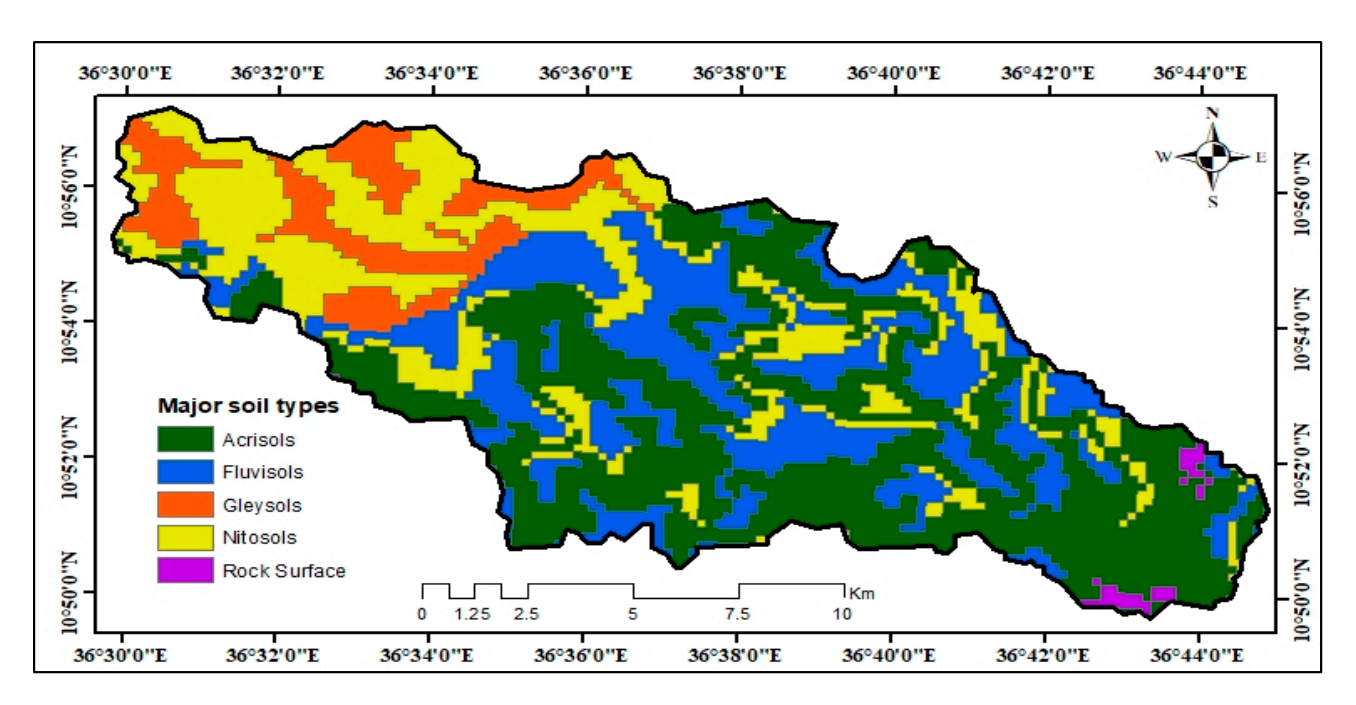


Figure 2. Major soil types of Dondor watershed [26].

2.2. Methods of Data Collections

2.2.1. Source of Data

Both primary and secondary sources of information were used in this investigation. Boundary maps of the districts, topographical maps, and satellite images were among the secondary data, while unpublished materials, office reports, and documents were the primary sources used for this study. As secondary sources of data, satellite imagery such as Landsat images, 20 m resolution Digital Elevation Models (DEMs), climate (rainfall) data, and soil data were used (Table 1).

Data Type	Resolution	Purpose	Source
DEM	20 m × 20 m	For hydrological analysis and calculating LS factor	https://earthexplorer.usgs.gov/, (accessed on 2 September 2024)
LANDSAT Satellite imagery	10/20/30	For LULC classification	https://earthexplorer.usgs.gov/, (accessed on 2 September 2024)
Rainfall (mm)	4 km × 4 km	Prepare rainfall map or R factor map	CHRS Data Portal available from 2003 to 2021 https://chrsdata.eng.uci.edu/, (accessed on 2 September 2024)
Soil type	1:50,000 scale	Prepare soil map or K factor map	FAO, 2007 [26]

Table 1. Spatial data requirements and specification for this study.

2.2.2. Sources of Data and Analysis Techniques for LULC Dynamics

The 10-year interval was chosen for the availability of image data for the study watershed. Moreover, in the study area there are a notable changes in land use and land cover over the past two decades, driven by soil erosion, urban expansion, agricultural expansion, and natural factors. And also based on the empirical studies, many studies on land use and land cover changes in similar contexts have used 10-year intervals, especially when they conduct their study at watershed level. We utilized Landsat-5, Landsat-7, and Sentinel-2 imagery with a 30 m spatial resolution, downloaded from the USGS Earth Explorer

Sustainability **2024**, 16, 10421 5 of 19

(http://earthexplorer.usgs.gov, accessed on 2 September 2024). To reduce atmospheric distortions, all images were captured during the dry season (January) when aerosols and water vapor are less likely to interfere with image quality. Atmospheric correction was conducted using the Dark Object Subtraction (DOS) method, which involved identifying dark objects and subtracting their reflectance values from each pixel across the years, correcting for atmospheric path radiance and enhancing surface clarity. For further cloud management, the Multi-Temporal Analysis method was employed. This technique combines images from different dates to identify and select pixels from the least cloud-covered areas, producing a clear composite image suitable for accurate interpretation (Table 2).

Table 2. Satellite images used in this study.

Satellite/Spacecraft ID	Sensor ID	Path/Row	Date of Acquisition	Spatial Resolution/ Grid Cell Size (m)	Cloud Cover (%)
Landsat-5	TM	170/053	31 January 2002	30 m	0
Landsat-7	ETM	170/052	5 January 2013	30 m	0
Sentinel-2		170/53	26 January 2023	10 m/20 m/60 m	0

Using supervised image classification methods, the LULC maps were created from different Landsat like Landsat-5, Landsat-7, and Sentinel-2 satellite images. For verification methods, Ground control points were gathered from Google Earth. Moreover, true color and false color compositions were used to classify analysis and interpret the image results. For Landsat data of TM and ETM sensors, Bands 3, 2, and 1 were used to build true-color composite images, whereas Bands 4, 3, and 2 were used to create false-color composite images. For Sentinel-2, true-color composite images were created using Bands 4, 3, and 2, and false-color composite images were created using Bands 5, 4, and 3. Based on the features of Landsat satellite images from 2002, 2013, and 2023, image classification techniques were used to identify four key land uses and land cover categories, including agricultural land, forest land, grass or grassland, and settlement or built-up areas in the Dondor watershed.

After identifying land use land cover types for 2003, 2013, and 2023, LULCC was computed between 2002–2013 and 2013–2023. Then we evaluated the accuracy assessment and analyzed the land use and land cover change matrix to quantify gains and losses of land use and land cover changes for different years. The accuracy of a classified map was evaluated and compared with reference data using an error matrix based on historical Google Earth data. User accuracy, producer accuracy, and overall accuracy were performed, and the result showed an overall accuracy of 77.83% with a Kappa coefficient greater than 0.75 for all years. For accuracy assessment, a total of 150 random points were generated from the four-land use land cover types in ArcMap 10.3 based on user image classification and Google Earth points for 2002, 2013, and 2023 (Table 3).

Table 3. Description of land use/land cover types.

No	Land Use Land Cover Classes	Description of Each Land Use Class
1	Agriculture Land	Areas of land plowed/prepared for growing various crops. This category includes areas currently under crop, fallow and land under preparation and rural homesteads
2	Forest Land	Forest areas covered with relatively tall and dense trees that formed nearly closed canopies around religious sites and at the upper escarpment of the watershed. This class also included plantation trees.

Sustainability **2024**, 16, 10421 6 of 19

Table 3. Cont.

No	Land Use Land Cover Classes	Description of Each Land Use Class
3	Grassland	Land predominately covered with grasses, and land units allocated as a source of animal feed. And also included some cases scattered trees mixed with grasses
4	Built-up area	Land being used for settlement/ urban land

2.2.3. Sources of Data and Analysis Techniques for Soil Loss Estimation

Identifying the spatial distribution of soil loss and sediment yield is imperative to tackle problems associated with soil loss and sediment yield by applying appropriate soil and water conservation strategies based on severity level [28]. Soil erosion is a function of the biophysical environment, comprising soil, climate, topography, ground cover, and interactions between them [29]. If the topography of the area is more sloped, the more runoff and thus infiltration reduces there are. According to [30], the RUSLE model uses six criteria to predict the mean annual soil erosion rate. In this way, the conundrum can be stated as:

$$A = R \times K \times LS \times C \times P \tag{1}$$

where

 $A = is the annual soil loss (tones ha^{-1} year^{-1})$

 $R = is rainfall erosivity factor (MJ mm <math>ha^{-1} h^{-1} year^{-1}$)

K = is soil erodibility factor (tones hour MJ⁻¹ mm⁻¹)

LS = is L and S are the slope length and steepness factors, respectively (dimensionless)

C = is Vegetation (cover) and Management Factor (dimensionless)

P = is the conservation practice factor or Support Practice Factor (dimensionless)

For estimating soil erosion, analysis of five factors as constant factors (LS factor, R factor, and K factor) and variable factors (C and P factors for 2002, 2013, and 2023) were used.

Rainfall-runoff erosivity factor (R)

The R-factor is an index that reflects the capacity of rainfall runoff to separate and transport soil particles that are experimentally determined by taking into account the intensity and maximum duration of rainfall in a specific area of interest [31]. It is linked to the quantity and rate of runoff, which can result in erosion, and it represents the impact of rainfall. For this study, the mean annual rainfall data which were available from 2003 to 2021 were used to calculate the rainfall-runoff erosivity factor (Figure 3). This study used gridded rainfall data at a spatial resolution of 4 km by 4 km, which was downloaded from CHRS Data Portal (https://chrsdata.eng.uci.edu/, accessed on 2 September 2024). Based on the available mean yearly rainfall data, [32] modified the model for the Ethiopian condition. Thus, the equation is as follows:

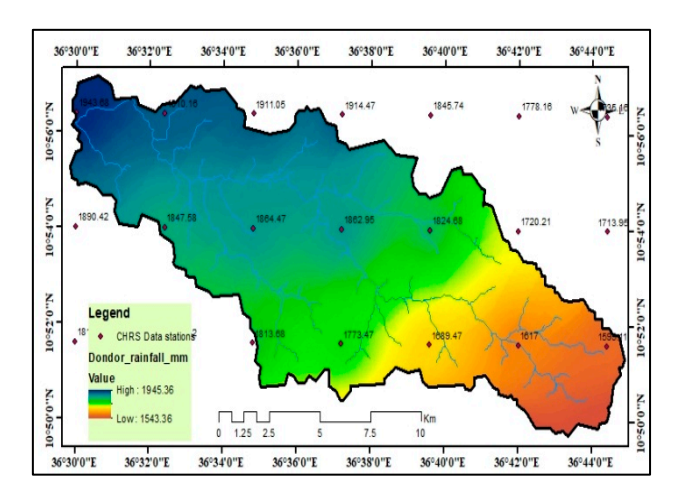
$$R = (0.562 \times P) - 8.12 \tag{2}$$

where

R = is rain fall erosivity factor and

P = is the available mean annual rainfall (mm) data.

Sustainability **2024**, 16, 10421 7 of 19



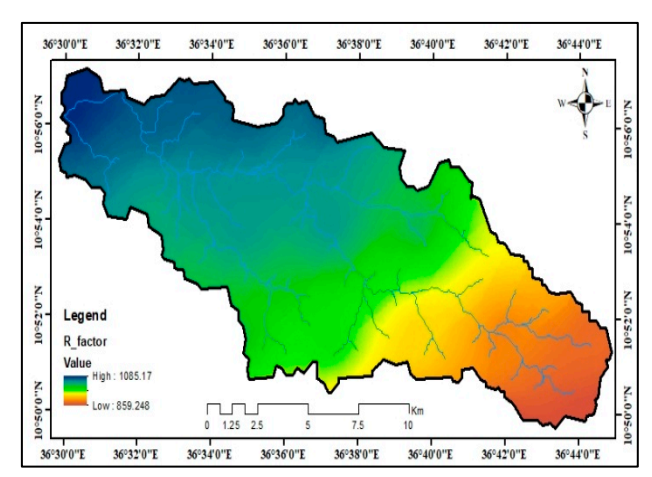
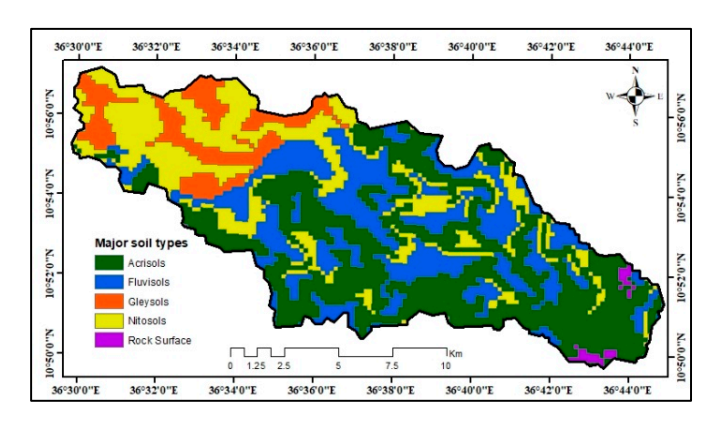


Figure 3. Rainfall and R factor map used for the RUSLE model.

Soil Data and Soil Erodibility Factor (K)

Soil erosion prediction relies on understanding soil erodibility [33]. Based on the quantity of rainfall and runoff input, the soil erodibility factor (K-factor) computes the susceptibility of soil particles or surface materials to transportation and detachment [30]. The main factors influencing soil erosion are associated with topography of the physical landscape, slope length and slope steepness, and the degree of disturbance, such as tillage. For this study, the major soil types obtained from [26] were used to calculate the soil erodibility factor. As per FAO soil map, the major soils in the study area are Acrisols, Fluvisols, Gleysols, Nitosols, and rock surface. The K values for Acrisols, Fluvisols, Gleysols, Nitosols, and Rock surface are 0.27, 0.3, 0.26, 0.25, and 0, respectively [32] (Figure 4).



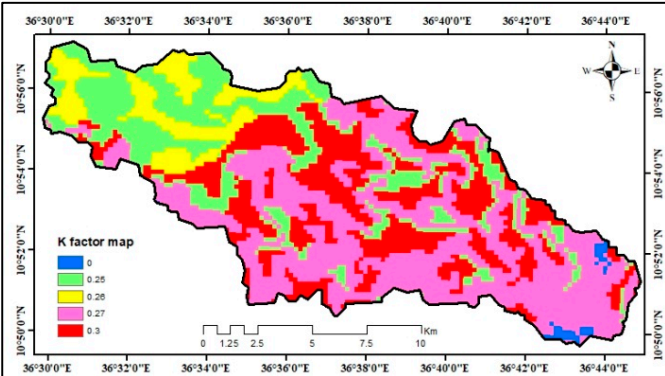


Figure 4. Soil types and K factor map used for the RUSLE model.

Topographic (slope length and steepness) Factors

In this study, a Digital Elevation Model (DEM) with a resolution of $20 \text{ m} \times 20 \text{ m}$ was employed to assess the topographic (L and S) variables. The topographic (LS) factors map for the Dondor watershed was developed using the DEM data (Figure 5). ArcGIS 10.3 was used to create the LS factor grid map and the research area's slope map (in degrees). The slope map of the study area (in degree) and the LS factor grid map were developed by using ArcGIS 10.3. Based on DEM, slope degree map and flow accumulation was generated. Put differently, ArcGIS 10.3 was used to calculate the flow accumulation and slope steepness from the DEM. Flow accumulation and slope maps were multiplied by using "Spatial Analyst Tool and Map Algebra Raster Calculator" in ArcGIS to calculate and map the slope length (LS factor) as shown in the below equation which was defined by [31]. Lastly, the

Sustainability **2024**, 16, 10421 8 of 19

result of LS map was used as an input data for RUSLE model to forecast soil loss in the study area.

S = (Flow Acc. \times Cell size/22.13)^{0.4} \times (sin (slope degree \times 0.01745)/0.0896)^{1.4} \times 1.4 (3)

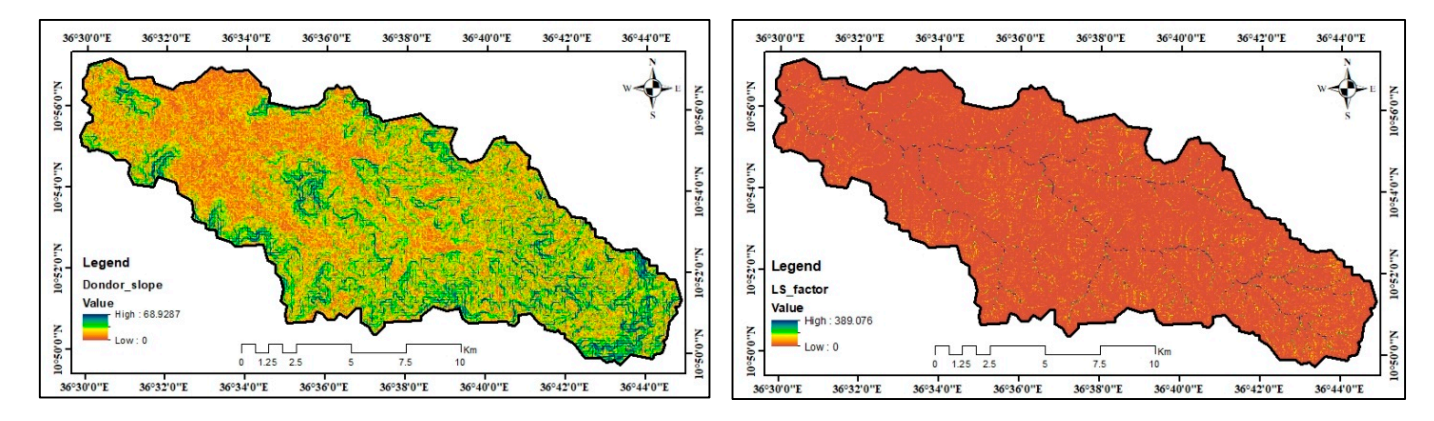


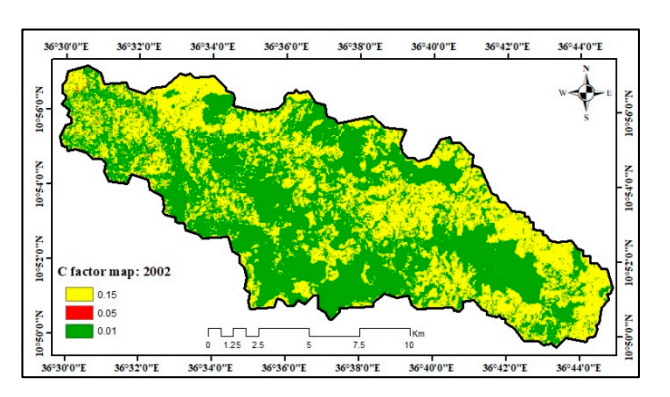
Figure 5. Slope and LS factor map used for the RUSLE model.

Management Factor (C-values) and Conservation Practice Factor (p-Values)

The land use and land cover types produced from the Landsat satellite images of 2002 (TM), 2013 (ETM), and 2023 (Sentinel-2A) were used to compute the C and P factor values for the Dondor watershed (Figure 6). Based on recommended values from earlier research, four main LULC categories were determined, and the matching C and P factor values were allocated for each land use land cover type. The LULC classes and the corresponding C and P variables in the study watershed were adopted from [32]. Eventually, a spatial distribution map was developed (Table 4).

Table 4. C and P factor values of different land use land cover classes.

LULC	Description	C Value	p Value
Agriculture	Areas used for crop cultivation, both annual and perennials	0.150	0.9
Forestland	Areas covered with dense growth of both natural and man-made trees	0.010	0.7
Grassland	Grassy areas predominantly covered with grasses	0.010	0.8
Built-up	Urban areas and other man-made structures	0.050	0.9
Source [32].			



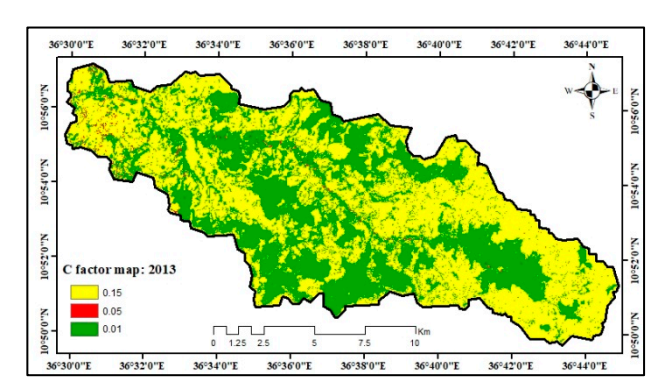


Figure 6. Cont.

Sustainability **2024**, 16, 10421 9 of 19

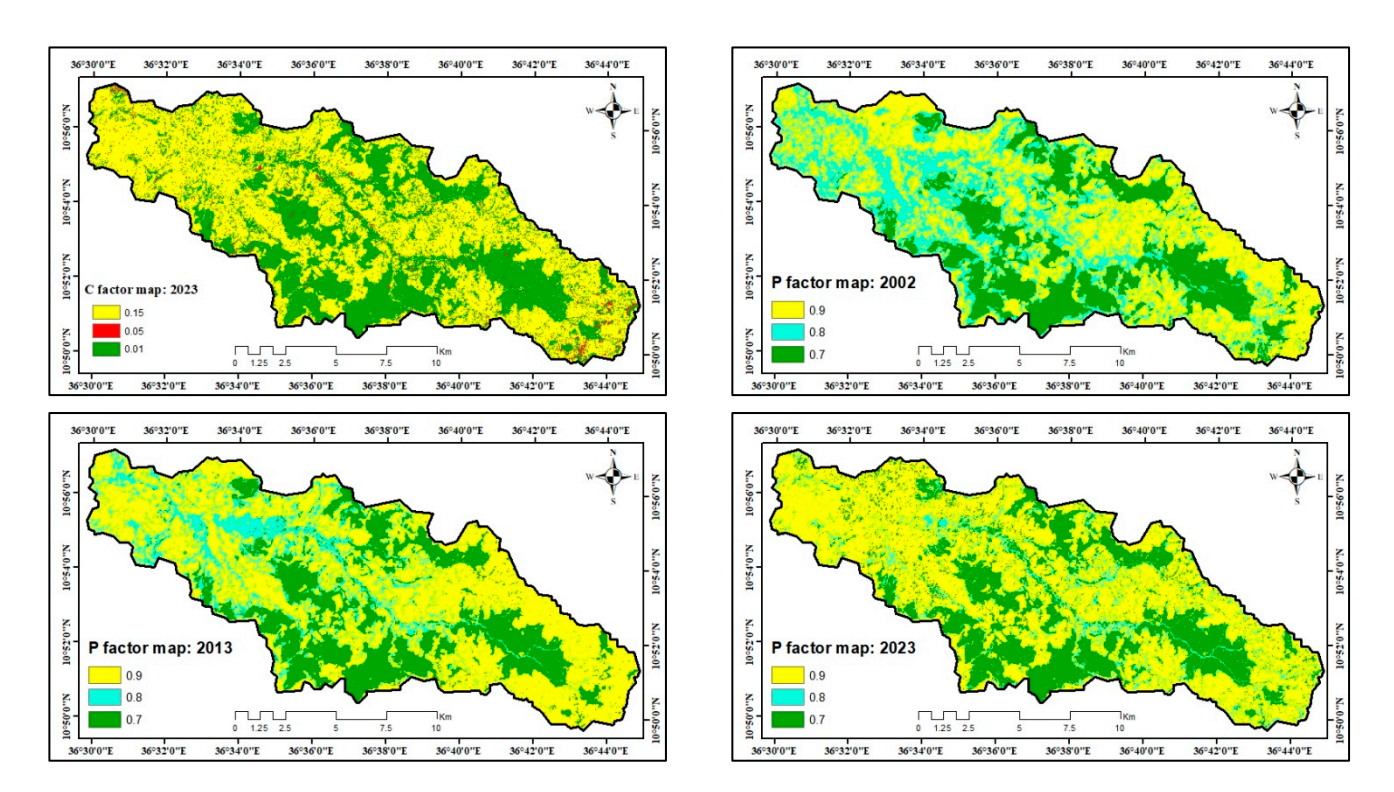


Figure 6. C factor and P factor map for 2002, 2013 and 2023 used for the RUSLE model.

All data were input into the RUSLE model, and the data resolutions were converted into grid cells of 30 m \times 30 m in a uniform size to estimate the annual soil erosion and to recognize its spatial distribution of soil loss in the watershed. There are five severity classes for the projected annual soil erosion (A). These include very slight (0–5 t ha⁻¹ year⁻¹), slight (5–11 t ha⁻¹ year⁻¹), moderate (11–30 t ha⁻¹ year⁻¹), severe (30–50 t ha⁻¹ year⁻¹), and very severe (>50 t ha⁻¹ year⁻¹) [34].

3. Results

3.1. Spatio-Temporal Dynamics of Land Use Land Cover Classification of Dondor Watershed

The produced land use and land cover maps and their area coverage in the Dondor watershed for the three reference years (2002, 2013, and 2023) are presented in Figure 7 and Table 5. Spatial and temporal variations in land cover classes and land use were analyzed for the two successive time periods (2013–2023 and 2002–2013) in the study area. Based on the land use and cover classification of the TM satellite image for 2002, agricultural land made up the largest portion of the study watershed, covering 8181.36 ha (43.49%), followed by grassland (32.17%) and forest land (24.24%). However, within the watershed, only 0.1% of the total area was developed or inhabited. The land use and cover classification for the year generated from 2013 Landsat-7 ETM sensor satellite image also showed that the Dondor watershed's total area was made up of 55.61% agricultural land (10,460.88 hectares), followed by forest land (25.80%), grassland (18.04%), and built-up area (0.56%). The 2023 Sentinel-2A satellite image analysis revealed that agriculture continued the dominant land use in the study area, occupying 59.10% of the total area, followed by forest land at 28.25% and grassland at 11.39%. Since 2002, agricultural land has consistently been the primary land cover in the Dondor watershed.

Sustainability **2024**, 16, 10421 10 of 19

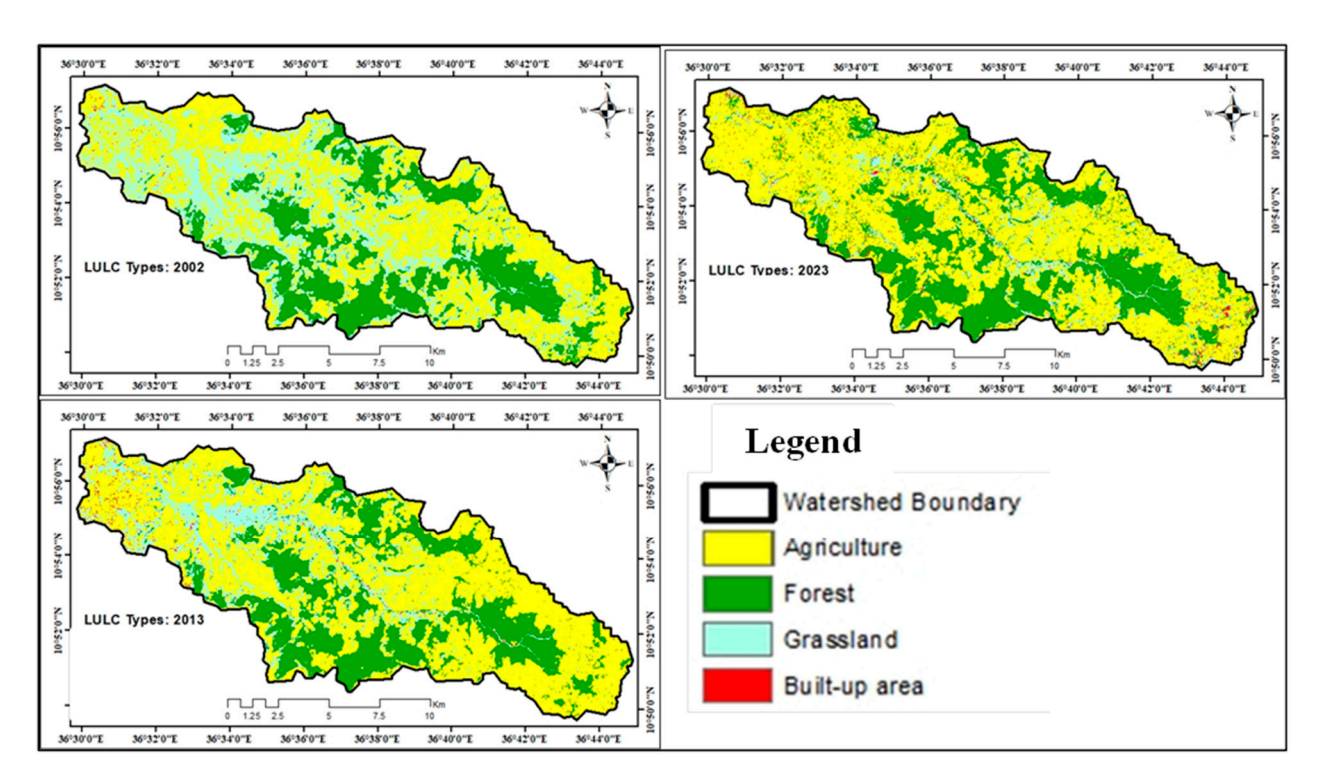


Figure 7. The Land Use and Land Cover (LULC) maps of the Dondor watershed are presented for three reference years: 2002, 2013, and 2023.

Land Use Land	Year:	2002	Year:	2013	Year: 2023	
Cover Types	Area (Ha)	Area (%)	Area (Ha)	Area (%)	Area (Ha)	Area (%)
Agriculture	8181.36	43.49	10,460.88	55.61	11,119.21	59.10
Forest	4560.39	24.24	4852.71	25.80	5315.34	28.25
Grassland	6051.96	32.17	3394.26	18.04	2141.94	11.39
Built-up area	18.72	0.10	104.58	0.56	236.67	1.26
Total	18,812.43	100	18,812.43	100.00	18,813.16	100.00

Accuracy Assessment of Land Use Land Cover Types from 2002 to 2023

An accuracy evaluation was conducted after image classification to determine how accurately each land use and land cover type was classified. The assessment was performed using Google Earth, which compared the classified map with reference data through an error matrix, utilizing historical photos from Google Earth for each year, as no previous aerial photographs were available for the study watershed. In ArcMap, a total of 150 random points were generated. Accuracy tests were performed for the user, producer, and overall accuracy. To determine the user's accuracy, the number of correctly classified pixels in each category was divided by the total number of pixels in that category (row total) of the classified image. The number of correctly classified pixels in each class (category) divided by the total number of pixels in the reference data that belong to that category (column total) is referred to as the producer's accuracy [35]. Overall accuracy is computed by dividing the total number of correctly classified pixels (i.e., the sum of the elements along the major diagonal) by the total number of reference pixels. It shows an overall result of the tabular error matrix. Google Earth represents a powerful and attractive source of positional data that can be used for investigation and preliminary studies with suitable accuracy and low cost. Images from Google Earth with high spatial resolution are free for the public and can be used directly in land use and land cover mapping in small geographical areas. After

Sustainability **2024**, 16, 10421 11 of 19

the image was classified, a set of 150 random points was generated in ArcMap (Toolbox >>> Data Management Tools >>>) (Feature Class >>> Create Random Points) (Tables 6–8).

Table 6. Accurac	y assessment of l	and use land	cover change: 2002.
-------------------------	-------------------	--------------	---------------------

		Referenced from Google Earth (2002)				Row	User/Individual
		Agriculture	Forest	Grassland	Built-Up	Total	Accuracy
	Agriculture	40	4	2	1	47	0.85
User Image (2002 Classification)	Forest	3	33	3	5	44	0.75
	Grassland	3	2	21	0	26	0.81
	Built-up area	2	1	2	28	33	0.85
Column Total		48	40	28	34	150	

 $\begin{array}{l} Total \ (overall) \ accuracy = (40 + 33 + 21 + 28)/150 \times 100 = 122/150 = 0.813 \times 100 = 81.3\%; \ K = 150(40 + 33 + 21 + 28) - [(48 \times 40) + (40 \times 33) + (28 \times 21) + (34 \times 28)]; \ (150)^2 - [(48 \times 40) + (40 \times 33) + (28 \times 21) + (34 \times 28)]; \ K = 150(122) - [(1920) + (1320) + (588) + (952)] = 18,300 - 4780 = 13,520 = 0.762; 22,500 - [(1920) + (1320) + (588) + (952)] = 22,500 - 4780 = 17,720. \end{array}$

Table 7. Accuracy assessment of land use land cover change: 2013.

		Refer	Referenced from Google Earth (2013)				User/Individual
		Agriculture Forest Grassland Built-Up Total					Accuracy
User Image (2013 Classification)	Agriculture	38	3	3	2	46	0.83
	Forest	0	34	3	1	38	0.89
	Grassland	2	2	18	1	23	0.78
	Built-up	4	2	3	34	43	0.79
Column Total		44	41	27	38	150	

K (Kappa coefficient) = 0.779. Accordingly, Kappa of 0.779 means there is 77.9% better agreement than by chance alone.

Table 8. Accuracy assessment of land use land cover change: 2023.

		Referenced from Google Earth (2023) Agriculture Forest Grassland Built-Up				Row	User/Individual
						Total	Accuracy
		46	2	2	2	52	0.88
User Image (2023 Classification)	Forest	2	30	2	2	36	0.83
	Grassland	2	2	25	2	31	0.81
	Built-up	1	3	2	25	31	0.81
Column Total		44	51	37	31	31	150

 $K \ (Kappa \ coefficient) = 0.794. \ Hence, Kappa \ of \ 0.794 \ means \ there \ is \ 79.4\% \ better \ agreement \ than \ by \ chance \ alone.$

Thus, 76.2% better agreement than would result from chance alone is indicated by a Kappa of 0.76. The study's accuracy results for users revealed that, in 2002, the minimum accuracy was 75% for forest land, while the maximum accuracy was 85% for built-up areas and farmland, which were correctly identified. The findings shown in Table 6 indicated that the overall accuracy and Kappa coefficients for the year 2002 were 81.3% and 76.2%, respectively.

3.2. The Trends and Conversions of Land Use Land Cover Changes in Dondor Watershed

Grassland land showed a declining tendency between 2002 and 2013, while built-up areas, forests, and agricultural land all showed growing trends. Over this time span, there was an increase of 2279.52 ha, 292.32 ha, and 85.86 ha in the total coverage of built-up area, agricultural land, and forest land, respectively. Nevertheless, between 2002 and 2013, there was a 2657.7 ha decrease in grassland land. In the meantime, the Dondor watershed's

Sustainability **2024**, 16, 10421 12 of 19

land use and land cover change trends revealed that, between 2013 and 2023, there was an increase of 658.33 ha, 462.63 ha, and 132.09 ha in agricultural land, forest land, and built-up area, respectively. Grassland, however, demonstrated a decline of 1252.32 hectares between 2013 and 2023. The annual rate of change from 2002 to 2013 showed an increase of 1.98 ha, 0.55 ha, and 7.46 ha for agricultural, forest, and grassland, respectively. Moreover, there was a decrease of 7.12 ha in grassland each year from 2002 to 2013. On the other hand, from 2013 to 2023, the annual rate of change demonstrated increases of 0.59 ha, 0.87 ha, and 5.58 ha for agricultural, forest, and built-up areas, respectively. In addition, from 2013 to 2023, there was a 5.85 ha annual decline in grassland (Table 9).

Table 9. Land use / l	land cover types and	their changes (ha)	in Dondor watershed.
------------------------------	----------------------	--------------------	----------------------

	2002 to 2013			2013 to 2023			2002 to 2023		
Land Use Land Cover Types	Changes (ha)	Rate of Change (ha)	Annual Rate of Change (ha year ⁻¹)	Changes (ha)	Rate of Change (ha)	Annual Rate of Change (ha year ⁻¹)	Changes (ha)	Rate of Change (ha)	Annual Rate of Change (ha year ⁻¹)
Agriculture	2279.52	21.79	1.98	658.33	5.92	0.59	2937.9	26.42	1.32
Forest	292.32	6.02	0.55	462.63	8.70	0.87	754.95	14.20	0.71
Grassland	-2657.7	-78.30	-7.12	-1252.32	-58.47	-5.85	-3910	-182.55	-9.13
Built-up area	85.86	82.10	7.46	132.09	55.81	5.58	217.95	92.09	4.60

The data and/or information on land use and land cover conversions from one category to another for the years 2002 to 2013 and 2013 to 2023 are presented in Table 10. The diagonal elements of the matrix stand for persistence, while the off-diagonal elements reflect category conversions. Change detection analyses showed that there were notable changes in LULC over the course of both time periods. Between 2002 and 2013, 67.39 ha, 894.10 ha, and 24.79 ha of agriculture land were converted to forest land, grassland, and built-up area, respectively. From 2002 to 2013, a total of 211.85 ha, 0.68 ha, and 144.80 ha of forest land were converted to built-up land, grassland, and farmland, respectively. Furthermore, from 2002 to 2013, 3096.17 ha, 567.36 ha, and 62.05 ha of grassland were converted to agriculture land, forest land, and built-up area, respectively. Throughout these times, some of the built-up area was also turned into agricultural land (13.80 ha) and grassland (1.91 ha). Between 2013 and 2023, 439.94 ha, 948.67 ha, and 119.57 ha of agriculture land were transformed into forest land, grassland, and built-up area, respectively. From 2013 to 2023, 220.75 ha, 194.47 ha, and 34.86 ha of forest land were converted to agriculture land, grassland, and built-up land, respectively. Moreover, from 2002 to 2013, 1874.05 ha, 476.66 ha, and 50.95 ha of grassland were converted to agriculture land, forest land, and built-up area, respectively. Furthermore, from 2013 to 2023, a portion of the built-up area was also converted to agriculture land (2.65 ha), forest land (3.30 ha), and grassland (24.35 ha), respectively.

Table 10. Land use and land cover change matrices of the Dondor watershed.

	2013										
	Row Labels	Agricultural	Forest	Grassland	Built-up	Grand Total					
_	Agriculture (ha)	7257.39	67.39	894.10	24.79	8243.67					
2002	Forest (ha)	211.85	4217.71	144.80	0.68	4575.04					
_	Grassland (ha)	3096.17	567.36	2230.12	62.05	5955.7					
	Built-up area (ha)	13.80	0.00	1.91	0.45	16.16					
	Grand Total	10,579.21	4852.46	3270.93	87.97	18,790.57					

			-	^	0 .
13	hı	Δ	1	"	Cont.

			2023			
	Agriculture (ha)	9070.84	439.94	948.67	119.57	10,579.02
	Forest (ha)	220.75	4401.95	194.47	34.86	4852.03
2013	Grassland (ha)	1874.05	476.66	868.88	50.95	3270.54
	Built-up area (ha)	2.65	3.30	24.35	57.60	87.9
	Grand Total	11,168.29	5321.85	2036.3	262.98	18,789.49

The coefficient of variance (CV), which represents the rate of change in the types of land cover and land use, is displayed in the table below (Table 11). A greater CV denotes a faster rate of change for both land cover and land use categories. Therefore, based on the CV values, the built-up areas, grassland, agricultural land, and forest land showed a quicker rate of change between 2002 and 2023.

Table 11. Coefficient of variance for land use and land cover types from 2002 to 2023.

LULC Types	2002 Area (Ha)	2013 Area (Ha)	2023 Area (Ha)	Standard Deviation (SD)	Mean or Average (M)	Coefficient of Variance (CV) = (S/M) × 100
Agriculture Land	8181.36	10,460.88	11,119.21	1258.77	9920.48	12.69
Forest Land	4560.39	4852.71	5315.34	310.81	4909.48	6.33
Grassland	6051.96	3394.26	2141.94	1630.27	3862.72	42.21
Built-up area	18.72	104.58	236.67	89.64	119.99	74.71

3.3. The Annual Soil Loss of Dondor Watershed Using RUSLE

From 2002 to 2023, the yearly rate of soil erosion in the Dondor watershed was calculated using the RUSLE model. Using the raster calculator and ArcGIS 10.3's spatial analysis capabilities, this analysis was carried out cell-by-cell. Ultimately, five severity classes were identified based on the estimated rate of soil erosion: very slight (0–5 t ha $^{-1}$ year $^{-1}$), slight (5–15 t ha $^{-1}$ year $^{-1}$), moderate (15–30 t ha $^{-1}$ year $^{-1}$), severe (30–50 t ha $^{-1}$ year $^{-1}$), and very severe (>50 t ha $^{-1}$ year $^{-1}$) (Figure 8, Table 12). The annual soil loss in the Dondor watershed ranged from 0 to 13,253.5 t ha $^{-1}$ year $^{-1}$ in 2002, 0 to 12,928.6 t ha $^{-1}$ year $^{-1}$ in 2013, and 0 to 13,253.5 t ha $^{-1}$ year $^{-1}$ in 2023, and the mean annual soil loss for the entire watershed was estimated at 4.98, 5.41, and 7.96 t ha $^{-1}$ year $^{-1}$ in 2002, 2013, and 2023, respectively. The amount of soil loss in Dondor watershed classified from the RUSLE model in 2002 showed that the majority of the study watershed soil loss was characterized as very slight soil erosion class, which accounted for 15,604.2 ha and contributed 83.17% of the total area, followed by slight soil loss (9.33%), moderate soil loss (3.62%), very severe soil loss (2.13%), and severe soil loss (1.74%) category or class.

Table 12. Soil erosion severity classes in the Dondor watershed from 2002 to 2023.

Soil Loss	Soil Loss	2002		20	13	2023	
Class	(t ha^{-1} $year^{-1}$)	Area (ha)	Area (%)	Area (ha)	Area (%)	Area (ha)	Area (%)
Very Slight	0 to 5	15,604.2	83.17	14,818.86	78.99	14,563.89	77.60
Slight	5 to 15	1750.86	9.33	2135.79	11.38	2273.58	12.11
Moderate	15 to 30	679.95	3.62	859.14	4.58	910.35	4.85
Severe	30 to 50	326.61	1.74	425.16	2.27	451.17	2.40
Very severe	> 50	399.69	2.13	522.09	2.78	568.89	3.03
Total		18,761.31	100	18,761.04	100	18,767.88	100

Sustainability **2024**, 16, 10421 14 of 19

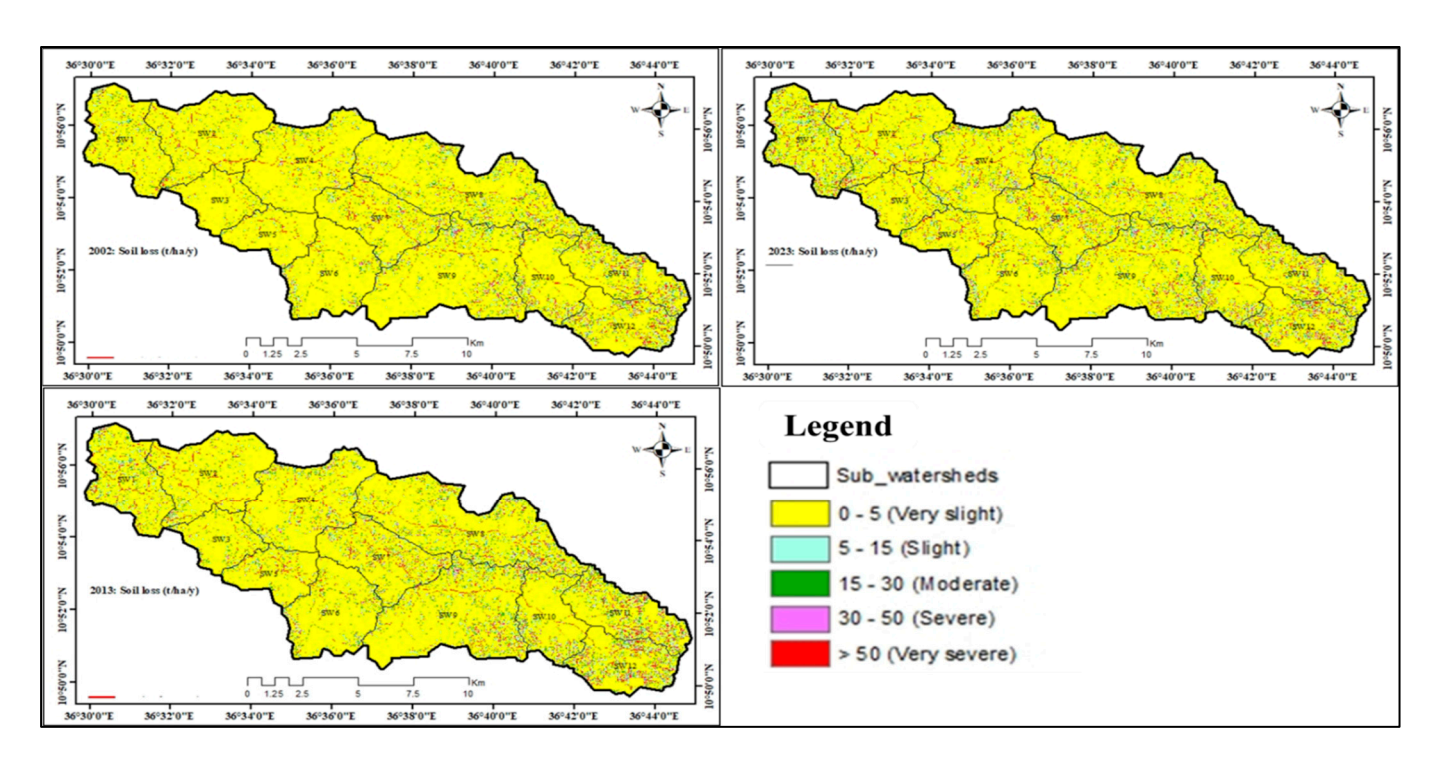


Figure 8. The spatial distributions of soil loss in the Dondor watershed for three reference years: 2002, 2013, and 2023.

However, the amount of soil loss in the Dondor watershed was classified in 2013 using the RUSLE model, which revealed that most of the soil loss in the study watershed was classified as very slight soil erosion class. This class accounted for 14,818.86 ha and contributed 78.99% of the total area. The other classes of soil loss were slight (11.38%), moderate (4.58%), very severe (2.78%), and severe (2.27%). The mean soil loss in the watershed increased from 2002 to 2013, possibly due to increased agricultural land and built-up areas and a decrease in grassland (Figure 8).

Analysis of soil loss in the Dondor watershed using the RUSLE model for 2023 revealed that the majority of the area continued to experience very slight erosion, covering 14,563.89 hectares (77.60% of the total). This was followed by slight (12.11%), moderate (4.85%), very severe (3.03%), and severe (2.40%) erosion. While very slight erosion had been the dominant category since 2002, the average soil loss increased over time, likely due to documented land use changes. Grasslands decreased, while built-up areas and agricultural lands expanded during this period.

Finally, the amount of soil erosion status in the study watershed was assessed from 2002 to 2023 using the RUSLE model. Our analysis revealed that over 85% of the entire area of the study watershed's soil loss was categorized as very slight soil erosion status. This low erosion rate was likely attributable to the substantial forest cover that persisted throughout the study period. The Dondor watershed predominantly experienced very slight soil erosion, accounting for over 88% of the total area. However, a notable shift occurred between 2002 and 2023, with a decrease in very slight erosion and a corresponding increase in moderate, severe, and very severe erosion rates. This suggests a transition from lower to higher erosion intensity levels. While the area affected by very slight erosion declined, the area with slight erosion expanded during the same period. The most severe soil loss, exceeding 50 t ha⁻¹ year⁻¹, was concentrated in the upper, steeper regions of the watershed and along river courses. Irrigation practices exacerbated soil loss along these pathways, contributing to a significant portion of the total erosion. This trend highlights the vulnerability of the watershed's steeper slopes and riparian zones to erosion, particularly under the influence of human activities like agriculture and irrigation.

3.4. Impacts of Land Use Land Cover Changes on Soil Loss

Soil erosion rates were highest in agricultural and built-up areas for all study years (2002, 2013, and 2023). In 2002, average soil loss rates were significantly higher in agricultural ($10.43 \text{ t ha}^{-1} \text{ year}^{-1}$) and built-up ($9.66 \text{ t ha}^{-1} \text{ year}^{-1}$) regions compared to forest ($1.01 \text{ t ha}^{-1} \text{ year}^{-1}$) and grassland ($2.66 \text{ t ha}^{-1} \text{ year}^{-1}$) areas. In 2002, the mean soil loss rates for agricultural, forest, grassland, and built-up areas were 10.43, 1.01, 2.66, and 9.66 t ha⁻¹ year⁻¹, respectively. Notably, both built-up and agricultural areas exceeded the watershed average of 4.98 t ha⁻¹ year⁻¹. By 2013, erosion rates had increased in built-up areas (16.22 t ha^{-1} year⁻¹) and decreased slightly in agricultural land (9.05 t ha^{-1} year⁻¹). Despite this, the combined average for these land uses remained higher than the watershed average (5.41 t ha^{-1} year⁻¹). In 2023, erosion rates continued to be significant in built-up areas (12.53 t ha⁻¹ year⁻¹) and agricultural land (10.44 t ha⁻¹ year⁻¹), surpassing the watershed average of 7.66 t ha⁻¹ year⁻¹. Throughout the study period, grassland and forest areas exhibited consistently lower erosion rates than cultivated land and the overall watershed. The rate of soil loss in built-up areas was generally comparable to or higher than that of agricultural land. Table 13 provides a detailed breakdown of soil erosion rates for each land use land cover class, with minimum values of zero indicating areas with no detectable erosion.

T 10		Agriculture	Forest	Grassland	Built-Up	Entire Watershed
Estimated Soil Loss in 2002	Maximum	13,253.48	307.35	10,954.51	1397.44	13,253.48
$(t ha^{-1} year^{-1})$	Mean	10.43	1.01	2.66	9.66	4.98
	SD	175.39	6.37	87.11	95.82	117.98
Estimated Soil	Maximum	12,928.58	734.22	785.39	1506.83	12,928.58
Loss in 2013	Mean	9.05	0.91	2.13	16.22	5.41
(t ha^{-1} year $^{-1}$)	SD	134.83	8.26	20.94	93.87	101.19
Estimated Soil	Maximum	13,253.48	8871.21	6314.08	3890.76	13,253.48
Loss in 2023	Mean	12.53	1.50	6.60	10.44	7.66
($t ha^{-1} year^{-1}$)	SD	188.34	67.79	89.79	117.50	145.19

Table 13. The amount of soil loss in different land use types for 2002, 2013, and 2023.

4. Discussion

4.1. Land Use/Land Cover Change

The Dondor watershed land use and land cover analysis from 2002 to 2023 shows significant changes, such as a steady rise in agricultural land and expansion of forested and in built-up regions, while grassland has drastically decreased. Several studies support these findings; for instance, Ref. [15] reported similar trends of increased agricultural land at the expense of forest cover in the Birr and Upper-Didesa watersheds, while [36] reported comparable changes in the Andassa watershed. Conversely, a sharp increase in forest land was observed in the Chemoga watershed due to community afforestation programs [37], and the expansion of eucalyptus plantations has been contributing to an important increase in the forest cover in Gilgel Abbay watershed [15]. The phenomenon of greening phases and reforestation efforts has also been documented, notably in the work of [38], which indicated a regeneration of previously degraded lands in the Ethiopian Highlands. This aligns with the Dondor watershed's increasing forest cover, suggesting that some areas are benefiting from concerted restoration efforts, although the degree of regeneration varies by region based on management practices and environmental conditions.

4.2. Impacts of Land Use Land Cover Changes on Soil Loss

In the Dondor watershed, the relatively low annual soil loss reflects a stable ecosystem in terms of soil conservation. This finding aligns with research conducted by [11] in the Yezat Watershed, northwestern Ethiopia, where projected soil loss varied between 7.2 t ha $^{-1}$ year $^{-1}$ in 2001 and 4.8 t ha $^{-1}$ year $^{-1}$ in 2015, a pattern of gradual improvement

likely due to land management interventions. This suggests that although both watersheds have been subject to efforts in land management, the Dondor watershed may have benefitted from better overall land cover or topographical advantages. Unlike the present study, Ref. [39] found a trend in the Rib watershed between 1986 and 2016 toward increased severe erosion and decreased milder forms. In contrast to this study, steeper slopes were identified in the Chemoga [40], Borena District [41], Koga [42], and Melaka [43] watersheds. This shows that these areas may be more susceptible to erosion due to their steeper terrain. The differences in erosion patterns and slope characteristics between the present study and previous research provide valuable context for understanding the erosion dynamics in the area.

The change in soil erosion rates in the Dondor watershed during the 2002–2023 periods is linked to an increase in erosion-prone LULC categories, such as agricultural land and built-up areas, and a reduction in vegetation cover, such as forests and grasslands, which are less vulnerable to erosion. Similar findings have been reported in other regions, including the Maithon Reservoir catchment in India (1989–2004) [44], Ethiopia's Central Rift Valley (1973–2006) [45], the Rib watershed in Ethiopia (1986–2016) [39], and the Andassa watershed in Ethiopia [36]. On the other hand, areas with vegetation cover show lower erosion risk, as vegetation stabilizes the soil and reduces erosion. This observation is consistent with findings from the Chemoga watershed [40] and the Central Rift Valley [45]. The relationship between LULC and estimated soil erosion was analyzed by overlaying LULC and soil erosion maps in the study area. This analysis serves as a valuable tool for monitoring changes in LULC patterns and assessing the associated risk of soil erosion [46,47].

4.3. Practical Implications for Land Use Management

This study highlights the expansion of agricultural land and built-up areas as major causes of soil erosion, with implications for conservation and land use management strategies in the Dondor watershed of the Blue Nile Basin. The rising erosion rates between 2002 and 2023 necessitate targeted interventions to prevent further degradation, particularly in zones with higher soil loss. Identifying areas with severe erosion is essential for agricultural experts to prioritize intervention activities, such as reforestation and sustainable agricultural practices. The findings inform policies aimed at enhancing soil conservation measures, particularly near river courses where intensified irrigation has exacerbated erosion.

The results emphasize the urgent need for targeted land management interventions in erosion-prone regions. Implementing conservation practices, such as terracing, agroforestry, and reforestation, can significantly mitigate soil loss. By integrating these findings into land use policies, stakeholders can address the increasing trend in soil erosion, prevent further degradation, and promote sustainable agricultural practices that align with conservation goals. Effective watershed management strategies are essential for balancing land use with ecological protection.

4.4. Research Limitations and Future Prospects

Using the RUSLE model, this study assessed how changes in land use and land cover (LULC) affected soil erosion between 2002 and 2023. Although some findings were obtained, there are still issues that need further investigation and improvement in future research. First, the data collection and processing have certain limitations. Higher-resolution satellite data and improved atmospheric correction techniques could enhance the accuracy of future assessments. Secondly, the RUSLE model has limitations, even though it was used in this research to simulate soil erosion. While this model is generally suitable for long-term soil erosion studies, its implementation may be less effective for small watersheds or on smaller slope scales. Its parameter settings are somewhat empirical, further contributing to uncertainties in the results. To improve the simulation capabilities of soil erosion processes at various scales, future research should consider incorporating more complex and precise erosion models, such as the SWAT model (Soil and Water Assessment Tool). Furthermore, this research did not adequately account for the dynamic effects of climate change, an

Sustainability **2024**, 16, 10421 17 of 19

important factor affecting soil erosion. Future investigations should integrate climate change scenarios to assess how shifting climatic conditions might affect soil erosion trends and to inform land use planning and ecological protection strategies more effectively.

5. Conclusions

The Dondor watershed has undergone significant land use/land cover transformations over the past two decades. Land used for agriculture has continuously dominated the landscape, but its area has expanded notably. On the other hand, forest land and built-up areas have increased while grassland has decreased. The watershed has witnessed substantial land cover conversions between different categories. Agricultural land has gained significant area, primarily at the expense of grassland. According to the analysis using the Revised Universal Soil Loss Equation (RUSLE), the mean annual soil loss gradually increased from 4.98 t ha⁻¹ year⁻¹ in 2002 to 7.96 t ha⁻¹ year⁻¹ in 2023. Areas near river courses, often associated with irrigation activities, have been identified as high soil loss zones. Regarding land use impact, farmland and built-up areas are major contributors to soil erosion, consistently exhibiting higher mean soil loss rates than the overall watershed average. To address soil erosion and maintain watershed health, this study recommends implementing targeted conservation strategies in areas with high soil loss, particularly near river courses and cultivated lands. A comprehensive approach that combines land use planning, erosion control strategies, and sustainable farming practices is essential to mitigate soil degradation and promote sustainable land management in the Dondor watershed.

Author Contributions: Conceptualization, L.B., Y.M., A.T., N.A. and H.B.; Methodology, L.B. and A.T.; Software, Y.M. and A.T.; Validation, H.B.; Formal analysis, A.T.; Investigation, L.B. and Y.M.; Resources, L.B. and A.T.; Data curation, Y.M. and A.T.; Writing—original draft, L.B. and Y.M.; Writing—review and editing, L.B., N.A. and H.B.; Visualization, L.B. and N.A.; Supervision and funding acquisition, H.B. All authors have read and agreed to the published version of the manuscript.

Funding: H.B. was supported by Natural Environment Research Council (NERC) through the National Centre for Earth Observation (NCEO), which also covered the article processing charge (APC) for publication.

Institutional Review Board Statement: Not applicable.

Informed Consent Statement: Not applicable.

Data Availability Statement: The manuscript contains all the necessary data.

Acknowledgments: The Agriculture and Rural Development Office of the Guangua District, as well as the respective chairpersons, are also highly acknowledged. The author's wishes to acknowledge the support from the University of Leicester's Institute for Environmental Futures, Space Park Leicester, for providing office space, internet access, and reference materials that facilitated this research.

Conflicts of Interest: The authors declare no competing interests.

References

- 1. Adhikary, P.P.; Tiwari, S.P.; Mandal, D.; Lakaria, B.L.; Madhu, M. Geospatial comparison of four models to predict soil erodibility in a semi-arid region of Central India. *Environ. Earth Sci.* **2014**, 72, 5049–5062. [CrossRef]
- 2. Haregeweyn, N.; Tesfaye, S.; Tsunekawa, A.; Tsubo, M.; Meshesha, D.T.; Adgo, E.; Elias, A. Dynamics of land use and land cover and its effects on hydrologic responses: Case study of the Gilgel Tekeze catchment in the highlands of Northern Ethiopia. *Environ. Monit. Assess.* 2015, 187, 4090. [CrossRef] [PubMed]
- 3. Meshesha, D.T.; Tsunekawa, A.; Tsubo, M.; Ali, S.A.; Nigussie Haregeweyn, N.H. Land-use change and its socio-environmental impact in Eastern Ethiopia's highland. *Reg. Environ. Change* **2014**, *14*, 757–768. [CrossRef]
- 4. Seutloali, K.E.; Beckedahl, H.R. A review of road-related soil erosion: An assessment of causes, evaluation techniques and available control measures. *Earth Sci. Res. J.* **2015**, *19*, 73–80. [CrossRef]
- 5. Abebe, Z.D.; Sewnet, M.A. Adoption of soil conservation practices in North Achefer district, Northwest Ethiopia. *Chin. J. Popul. Resour. Environ.* **2017**, *12*, 261–268. [CrossRef]
- 6. Leh, M.; Bajwa, S.; Chaubey, I. Impact of land use change on erosion risk: An integrated remote sensing, geographic information system and modeling methodology. *Land Degrad. Dev.* **2011**, 24, 409–421. [CrossRef]

- 7. Doe, J.; Smith, J. Deforestation Trends in East Africa. Environ. Conserv. J. 2020, 10, 123–135.
- 8. Balasubramanian, A. *Soil Erosion–Causes and Effects*; Centre for Advanced Studies in Earth Science, University of Mysore: Mysore, India, 2017.
- 9. Ayalew, G. Geographic information system-based soil loss and sediment estimation in zingin watershed for conservation planning, highlands of Ethiopia. *World Appl. Sci. J.* **2015**, *33*, 69–79. [CrossRef]
- 10. Nigatu, A. Impact of Land Use Land Cover Change on Soil Erosion Risk: The Case of Denki River Catchment of Ankober District. Master's Thesis, Addis Ababa University, Addis Ababa, Ethiopia, 2014.
- 11. Tadesse, L.; Suryabhagavan, K.V.; Sridhar, G.; Legesse, G. Land use and land cover changes and Soil erosion in Yezat Watershed, North Western Ethiopia. *Int. Soil Water Conserv. Res.* **2017**, *5*, 85–94. [CrossRef]
- 12. Teshome, A.; De Graaff, J.; Kassie, M. Household-level determinants of soil and water conservation adoption phases: Evidence from North-Western Ethiopian highlands. *Environ. Manag.* **2016**, *57*, 620–636. [CrossRef]
- 13. Selassie, Y.G.; Amede, T. Investing in land and water management practices in the Ethiopian highlands. Short- or long-term benefits. In *Challenges and Opportunities for Agricultural Intensification of the Humid Highland Systems of Sub-Saharan Africa*; Vanlauwe, B., Van Asten, P., Blomme, G., Eds.; Springer International Publishing: Cham, Switzerland, 2014.
- 14. Haregeweyn, N.; Tsunekawa, A.; Poesen, J.; Tsubo, M.; Meshesha, D.T.; Fenta, A.A.; Nyssen, J.; Adgo, E. Comprehensive assessment of soil erosion risk for better land use planning in river basins: Case study of the Upper Blue Nile River. *Sci. Total Environ.* 2017, 574, 95–108. [CrossRef] [PubMed]
- 15. Gebrehiwot, S.G.; Bewket, W.; Bishop, K.; Gärdenäs, A.I. Forest covers change over four decades in the Blue Nile Basin, Ethiopia: Comparison of three watersheds. *Reg. Environ. Change* **2014**, *14*, 253–266. [CrossRef]
- Asres, R.S.; Tilahun, S.A.; Ayele, G.T.; Melesse, A.M. Analyses of land use/land cover change dynamics in the upland watersheds
 of Upper Blue Nile Basin. In *Landscape Dynamics, Soils and Hydrological Processes in Varied Climates*; Springer International
 Publishing: Cham, Switzerland, 2016; pp. 73–91.
- 17. Ganasri, B.P.; Ramesh, H. Assessment of soil erosion by RUSLE model using remote sensing and GIS—A case study of Nethravathi Basin. *Geosci. Front.* **2016**, *7*, 953–961. [CrossRef]
- 18. Farhan, Y.; Nawaiseh, S. Spatial assessment of soil erosion risk using RUSLE and GIS techniques. Environ. *Earth Sci.* **2015**, 74, 4649–4669. [CrossRef]
- 19. Fernández, C.; Vega, J.A. Evaluation of RUSLE and PESERA models for predicting soil erosion losses in the first year after wildfire in NW Spain. *Geoderma* **2016**, *273*, 64–72. [CrossRef]
- 20. Amare, A.; Simane, B. Climate change induced vulnerability of smallholder farmers: Agroecology-based analysis in the Muger sub-basin of the upper Blue-Nile basin of Ethiopia. *Am. J. Clim. Chang.* **2017**, *6*, 668–693. [CrossRef]
- 21. Tolessa, T.; Senbeta, F.; Kidane, M. The impact of land use/land cover change on ecosystem services in the central highlands of Ethiopia. *Ecosyst. Serv.* **2017**, *23*, 47–54. [CrossRef]
- 22. Gashaw, T.; Tulu, T.; Argaw, M.; Worqlul, A.W.; Tolessa, T.; Kindu, M. Estimating the impacts of land use/land cover changes on Ecosystem Service Values: The case of the Andassa watershed in the Upper Blue Nile basin of Ethiopia. *Ecosyst. Serv.* 2018, 31, 219–228. [CrossRef]
- 23. Wondie, M.; Mekuria, W. Planting of Acacia decurrens and dynamics of land cover change in Fagita Lekoma District in the Northwestern Highlands of Ethiopia. *Mt. Res. Dev.* **2018**, *38*, 230–239. [CrossRef]
- 24. Lemenih, M.; Kassa, H. Re-greening Ethiopia: History, challenges and lessons. Forests 2014, 5, 1717–1730. [CrossRef]
- 25. Hurni, H. Degradation and Conservation of the Resources in the Ethiopian Highlands. Int. Mt. Soc. 1998, 8, 123–130. [CrossRef]
- 26. FAO. *The State of Food and Agriculture: Paying Farmers for Environmental Services*; Agricultural Development Economics Division (ESA), FAO: Rome, Italy, 2007. Available online: www.fao.org/docrep/010/a1200e/a1200e00.htm (accessed on 2 September 2024).
- 27. Guangua District Agricultural Office Annual Report. 2020.
- 28. Kidane, M.; Bezie, A.; Kesete, N.; Tolessa, T. The impact of land use and land cover (LULC) dynamics on soil erosion and sediment yield in Ethiopia. *Heliyon* **2019**, *5*, e02981. [CrossRef] [PubMed]
- 29. Tamene, L.; Adimassu, Z.; Aynekulu, E.; Yaekob, T. Estimating landscape susceptibility to soil erosion using a GIS-based approach in Northern Ethiopia. *Int. Soil Water Conserv. Res.* **2017**, *5*, 221–230. [CrossRef]
- 30. Renard, K.G. Predicting soil erosion by water: A guide to conservation planning with the Revised Universal Soil Loss Equation (RUSLE). *Agric. Handb.* **1997**, 703, 25–28.
- 31. Wischmeier, W.H.; Smith, D.D. *Predicting Rainfall Erosion Losses: A Guide to Conservation Planning, Handbook No. 537*; United States Department of Agriculture: Washington, DC, USA, 1978.
- 32. Hurni, H. Erosion-productivity-conservation systems in Ethiopia. In Proceedings of the 4th International Conference on Soil Conservation, Maracay, Venezuela, 3–9 November 1985; pp. 654–674.
- 33. Wang, B.; Zheng, F.; Römkens, M.J.; Darboux, F. Soil erodibility for water erosion: A perspective and Chinese experiences. *Geomorphology* **2013**, *187*, 1–10. [CrossRef]
- 34. Nigussie, Z.; Tsunekawa, A.; Haregeweyn, N.; Adgo, E.; Nohmi, M.; Tsubo, M.; Aklog, D.; Meshesha, D.T.; Abele, S. Factors influencing small-scale farmers' adoption of sustainable land management technologies in north-western Ethiopia. *Land Use Policy* **2018**, *67*, 57–64. [CrossRef]
- 35. Congalton, R.G.; Green, K. Assessing the Accuracy of Remotely Sensed Data: Principles and practices; Lewis Publishers: New York, NY, USA, 1999.

36. Gashaw, T.; Tulu, T.; Aragaw, M.; Worqlul, A.W. Evaluation and prediction of land use/land cover changes in the Andassa watershed, Blue Nile Basin, Ethiopia. *Environ. Syst. Res.* 2017. 6, 17. [CrossRef]

- 37. Bewket, W. Land cover dynamics since the 1950s in Chemoga watershed, Blue Nile basin, Ethiopia. *Mt. Res. Dev.* **2002**, 22, 263–269. [CrossRef]
- 38. Nyssen, J.; Haile, M.; Naudts, J.; Munro, N.; Poesen, J.; Moeyersons, J.; Frankl, A.; Deckers, J.; Pankhurst, R. Desertification? Northern Ethiopia re-photographed after 140 years. *Sci. Total Environ.* **2008**, 407, 2749–2755. [CrossRef]
- 39. Moges, D.M.; Bhat, H.G. Integration of geospatial technologies with RUSLE for analysis of land use/cover change impact on soil erosion: Case study in Rib watershed, north-western highland Ethiopia. *Environ. Earth Sci.* **2017**, *76*, 765. [CrossRef]
- 40. Bewket, W.; Teferi, E. Assessment of soil erosion hazard and prioritization for treatment at the watershed level: Case study in the Chemoga watershed, Blue Nile basin, Ethiopia. *Land Degrad. Dev.* **2009**, 20, 609–622. [CrossRef]
- 41. Shiferaw, A. Estimating soil loss rates for soil conservation planning in the Borena District of South Wollo highlands, Ethiopia. *J. Sustain. Dev. Afr.* **2011**, *13*, 87–106.
- 42. Sewnet, H.; Sewnet, A. Soil loss estimation using GIS and Remote sensing techniques: A case of Koga watershed, Northwestern Ethiopia. *Int. Soil Water Conserv. Res.* **2016**, *4*, 126–136.
- 43. Mekuriaw, A. Assessing the effectiveness of land resource management practices on erosion and vegetative cover using GIS and remote sensing techniques in Melaka watershed, Ethiopia. *Environ. Syst. Res.* **2017**, *6*, 16. [CrossRef]
- 44. Sharma, A.; Tiwari, K.N.; Bhadoria, P.B.S. Effect of land use land cover change on soil erosion potential in an agricultural watershed. *Environ. Monit. Assess.* **2011**, *173*, 789–801. [CrossRef] [PubMed]
- 45. Meshesha, D.T.; Tsunekawa, A.; Tsubo, M.; Haregeweyn, N. Dynamics and hotspots of soil erosion and management scenarios of the Central Rift Valley of Ethiopia. *Int. J. Sed. Res.* **2012**, 27, 84–99. [CrossRef]
- 46. Marondedze, A.K.; Schütt, B. Assessment of soil erosion using the RUSLE model for the Epworth district of the Harare Metropolitan province, Zimbabwe. *Sustainability* **2020**, *12*, 8531. [CrossRef]
- 47. Khosrokhani, M.; Pradhan, B. Spatio-temporal assessment of soil erosion at Kuala Lumpur Metropolitan city using remote sensing data and GIS. *Geomat. Nat. Hazards Risk* **2014**, *5*, 252–270. [CrossRef]

Disclaimer/Publisher's Note: The statements, opinions and data contained in all publications are solely those of the individual author(s) and contributor(s) and not of MDPI and/or the editor(s). MDPI and/or the editor(s) disclaim responsibility for any injury to people or property resulting from any ideas, methods, instructions or products referred to in the content.